Metabolomic Analysis via Reversed-Phase Ion-Pairing Liquid Chromatography Coupled to a Stand Alone Orbitrap Mass Spectrometer

ARTICLE *in* ANALYTICAL CHEMISTRY · MARCH 2010

Impact Factor: 5.64 · DOI: 10.1021/ac902837x · Source: PubMed

6 AUTHORS, INCLUDING:

Wenyun Lu
Princeton University
73 PUBLICATIONS **2,421** CITATIONS
SEE PROFILE

Michelle F Clasquin
Agios Pharmaceuticals
4 PUBLICATIONS **313** CITATIONS
SEE PROFILE

Eugene Melamud
23 PUBLICATIONS **1,684** CITATIONS
SEE PROFILE

Amy A Caudy
University of Toronto
50 PUBLICATIONS **9,069** CITATIONS
SEE PROFILE

Anal. Chem. **2010,** *82,* 3212–3221

Metabolomic Analysis via Reversed-Phase Ion-Pairing Liquid Chromatography Coupled to a Stand Alone Orbitrap Mass Spectrometer

Wenyun Lu, Michelle F. Clasquin, Eugene Melamud, Daniel Amador-Noguez, Amy A. Caudy, and Joshua D. Rabinowitz*

Lewis-Sigler Institute for Integrative Genomics and Department of Chemistry Princeton University, Princeton, New Jersey 08544

We present a liquid chromatography−mass spectrometry (LC−MS) method that capitalizes on the mass-resolving power of the orbitrap to enable sensitive and specific measurement of known and unanticipated metabolites in parallel, with a focus on water-soluble species involved in core metabolism. The reversed phase LC method, with a cycle time 25 min, involves a water−methanol gradient on a C18 column with tributylamine as the ion pairing agent. The MS portion involves full scans from 85 to 1000 *m/z* at 1 Hz and 100 000 resolution in negative ion mode on a stand alone orbitrap ("Exactive"). The median limit of detection, across 80 metabolite standards, was 5 ng/mL with the linear range typically ≥100-fold. For both standards and a cellular extract from *Saccharomyces cerevisiae* (Baker's yeast), the median inter-run relative standard deviation in peak intensity was 8%. In yeast exact, we detected 137 known compounds, whose ^{13}C-labeling patterns could also be tracked to probe metabolic flux. In yeast engineered to lack a gene of unknown function (*YKL215C*), we observed accumulation of an ion of *m/z* 128.0351, which we subsequently confirmed to be oxoproline, resulting in annotation of *YKL215C* as an oxoprolinase. These examples demonstrate the suitability of the present method for quantitative metabolomics, fluxomics, and discovery metabolite profiling.

A key driver of the use of liquid chromatography−mass spectrometry (LC−MS) for metabolomics has been technological advances in instrumentation. On the chromatography side, these include the use of ultraperformance liquid chromatography (UPLC) to drive mobile phase through columns packed with small particles.[1−3] On the mass spectrometry side, particularly significant progress been in capabilities for affordable, high-resolution full scan MS analysis using time-of-flight[4] and orbitrap-based mass spectrometers.[5]

The orbitrap is a mass analyzer that dynamically traps ions in an electric field formed between a central spindle electrode and an outer barrel electrode.[6,7] Ions circulate around the inner electrode with an axial frequency that is directly related to mass-to-charge ratio (*m/z*). Time domain transients are detected and converted to mass spectra through Fourier transformation, analogous to Fourier transform ion cyclotron resonance (FTICR) but without a magnet. The orbitrap mass analyzer typically has a working resolution of ∼100 000 at *m/z* 200. Resolution is scan-time dependent, with longer scan times yielding higher resolution. The resolution is higher than that of most time-of-flight instruments (∼10 000 resolution)[4,8] and approaches that of FTICR (∼100 000−1 000 000 resolution).[9,10]

The first commercial instrument involving an orbitrap mass analyzer was a hybrid linear ion trap-orbitrap.[11] This instrument has proven to be a powerful tool in proteomics.[12] Its typical operation mode involves acquiring high-resolution full scan spectra in the orbitrap, while simultaneously conducting data-dependent MS/MS in the ion trap. The full scan data are used for peptide quantitation, with the tandem mass spectrometry (MS/MS) data used for peptide identification. A related strategy can be applied to small molecules, involving (1) quantitation of targeted compounds by selection of their masses from high-resolution full scan data, combined with (2) full scan screening in search of unknown compounds, followed by MS^n analysis to facilitate their identification.[13] Unlike for peptides, however, MS^n analysis alone is generally not adequate for identification of unknown metabo-

* To whom correspondence should be addressed. Joshua D. Rabinowitz, M.D., Ph.D., Lewis-Sigler Institute for Integrative Genomics, 241 Carl Icahn Laboratory, Princeton University, Princeton, NJ 08544. Phone: (609) 258-8985. Fax: (609) 258-3565. E-mail: joshr@genomics.princeton.edu.

(1) Wilson, I. D.; Nicholson, J. K.; Castro-Perez, J.; Granger, J. H.; Johnson, K. A.; Smith, B. W.; Plumb, R. S. *J. Proteome Res.* **2005**, *4*, 591–598.
(2) Yu, K.; Little, D.; Plumb, R.; Smith, B. *Rapid Commun. Mass Spectrom.* **2006**, *20*, 544–552.
(3) Nguyen, D. T. T.; Guillarme, D.; Rudaz, S.; Veuthey, J. L. *J. Sep. Sci.* **2006**, *29*, 1836–1848.
(4) Stroh, J. G.; Petucci, C. J.; Brecker, S. J.; Huang, N.; Lau, J. M. *J. Am. Soc. Mass Spectrom.* **2007**, *18*, 1612–1616.
(5) Breitling, R.; Pitt, A. R.; Barrett, M. P. *Trends Biotechnol.* **2006**, *24*, 543–548.
(6) Makarov, A. *Anal. Chem.* **2000**, *72*, 1156–1162.
(7) Hu, Q. Z.; Noll, R. J.; Li, H. Y.; Makarov, A.; Hardman, M.; Cooks, R. G. *J. Mass Spectrom.* **2005**, *40*, 430–443.
(8) van der Heeft, E.; Bolck, Y. J. C.; Beumer, B.; Nijrolder, A.; Stolker, A. A. M.; Nielen, M. W. F. *J. Am. Soc. Mass Spectrom.* **2009**, *20*, 451–463.
(9) Feng, X.; Siegel, M. M. *Anal. Bioanal. Chem.* **2007**, *389*, 1341–1363.
(10) Schaub, T. M.; Hendrickson, C. L.; Horning, S.; Quinn, J. P.; Senko, M. W.; Marshall, A. G. *Anal. Chem.* **2008**, *80*, 3985–3990.
(11) Makarov, A.; Denisov, E.; Kholomeev, A.; Baischun, W.; Lange, O.; Strupat, K.; Horning, S. *Anal. Chem.* **2006**, *78*, 2113–2120.
(12) Han, X. M.; Aslanian, A.; Yates, J. R. *Curr. Opin. Chem. Biol.* **2008**, *12*, 483–490.
(13) Hogenboom, A. C.; van Leerdam, J. A.; de Voogt, P. *J. Chromatogr., A* **2009**, *1216*, 510–519.

10.1021/ac902837x
Published on Web 03/29/2010

lites. Areas of application of the hydrid linear ion trap-orbitrap in small molecule analysis have included metabolites from microbes,[14] plants,[15] and animals.[16,17]

The scientific community continues pushing for instruments with high performance but modest cost. Recently a benchtop orbitrap mass spectrometer, marketed as "Exactive", was introduced by ThermoFisher Scientific.[18−20] This stand-alone mass analyzer, without the ion trap in the front, was designed mainly for high-accuracy, high-resolution full scans. The cost is roughly one-half that of its hybrid counterpart, rendering the instrument more accessible for ordinary laboratories. Here we couple this stand-alone orbitrap instrument to reversed-phase, ion-pairing liquid chromatography via electrospray ionization to analyze the cellular metabolome. Key characteristics of the resulting LC−MS method include fast analysis due to the use of a small particle column, effective quantitation of a broad range of known cellular metabolites, and simultaneous detection also of unanticipated metabolites via untargeted analysis. We evaluate the quantitative performance of the method using both metabolite standards and microbial extracts, including in the presence of isotopic labeling. We also highlight the method's potential to identify unanticipated metabolites and thereby to assign metabolic roles to genes of unknown function.

EXPERIMENTAL SECTION

Chemicals, Reagents, and Media Components. HPLC-grade water and methanol (OmniSolv, EMD Chemical) were obtained through VWR International (West Chester, PA). The majority of the metabolite standards (see the Supporting Information, Table S-1 and S-2), as well as tributylamine, acetic acid, and all media components, were obtained through Sigma-Aldrich (St. Louis, MO). Additional metabolite standards were obtained from the Human Metabolome Database.[21] Uniformly ^{13}C-D-Glucose (99%) and ^{15}N-NH_4Cl were obtained from Cambridge Isotope Laboratories (Andover, MA). Polytyrosine calibration solution was obtained from ThermoFisher Scientific (San Jose, CA). (*S*)-(−)-2-Pyrrolidone-5-carboxylic acid (98%) was purchased through Acros Organics, New Jersey.

Escherichia coli were grown in Gutnick minimal salt media:[22] KH_2PO_4, 4.7 g/L; K_2HPO_4, 0.5 g/L; K_2SO_4, 1 g/L; $MgSO_4 \cdot 7H_2O$, 0.1 g/L; NH_4Cl, 10 mM; and glucose, 4 g/L. The Baker's yeast *Saccharomyces cerevisiae* was grown in yeast nitrogen base (YNB) without amino acids (Difco, Detroit, MI) with 20 g/L glucose.

LC−MS Instrumentation and Method Development. The complete LC−MS platform consists of Accela U-HPLC system with quaternary pumps, an HTC PAL autosampler (CTC Analytics AG, Zwingen, Switchland), a Keystone hot pocket column heater, and an Exactive orbitrap mass spectrometer (all from ThermoFisher Scientific, San Jose, CA, unless otherwise noted), controlled by Xcalibur 2.1 software. Liquid chromatography separation was achieved on a Synergy Hydro-RP column (100 mm × 2 mm, 2.5 μm particle size, Phenomenex, Torrance, CA), using reversed-phase chromatography with the ion pairing agent tributylamine in the aqueous mobile phase to enhance retention and separation.[23−25] The present LC method is a modified version of a method originally described in ref 23 with the present method employing a smaller particle size column (2.5 μm instead of 4 μm) to reduce peak widths and expedite analysis. The total run time is 25 min (versus 80 min for the original method). The flow rate is 200 μL/min. Solvent A is 97:3 water/methanol with 10 mM tributylamine and 15 mM acetic acid; solvent B is methanol. The gradient is 0 min, 0% B; 2.5 min, 0% B; 5 min, 20% B; 7.5 min, 20% B; 13 min, 55% B; 15.5 min, 95% B; 18.5 min, 95% B; 19 min, 0% B; 25 min, 0% B. Other LC parameters are autosampler temperature 4 °C, injection volume 10 μL, and column temperature 25 °C.

An electrospray ionization interface was used to direct column eluent to the mass spectrometer. Because the ion pairing agent tributylamine will cause ion suppression in positive mode, the instrument was operated in negative mode only. Initial instrument optimization (tuning) was done by infusing a mixture of malate (m/z 133.0142), ATP (m/z 505.9885), and coenzyme A (m/z 766.1079), each at 1 μg/mL at a flow rate of 200 μg/mL, using a 11Plus syringe pump (Harvard Apparatus, Boston, MA). Various instrumental settings were optimized to maximize the signal with the final parameters as follows: sheath gas flow rate 25 (arbitrary units), auxiliary gas flow rate 8 (arbitrary units), sweep gas flow rate 3 (arbitrary units), spray voltage 3 kV, capillary temperature 325 °C, capillary voltage −50 V, tube lens voltage −100 V. The instrument was mass calibrated using the polytyrosine-1,3,6 standards every 3 days.

The Exactive mass spectrometer has a maximum scan range of m/z 50−4000. For the study of small molecule metabolites, of particular interest is the low mass range (m/z 85−1000). In preliminary experiments, we found that the high amount of phosphate and sulfate in typical cellular media adversely impact analysis, apparently due to a combination of ion suppression at the ion source and space-charge effects inside the orbitrap. To mitigate the latter, during the LC segments at which phosphate ($H_2PO_4^-$, m/z 96.9696, ∼6 min) and sulfate (HSO_4^-, m/z 96.9601, ∼13 min) elute, we chose a lower scan limit of $\geq m/z$ 100 (rather than m/z 85) to reduce the accumulation of phosphate and sulfate ions in the orbitrap. Although the scan limit does not provide high-resolution mass filtration, ions

(14) Herebian, D.; Zuhlke, S.; Lamshoft, M.; Spiteller, M. *J. Sep. Sci.* **2009**, *32*, 939–948.
(15) Herebian, D.; Choi, J. H.; Abd El-Aty, A. M.; Shim, J. H.; Spiteller, M. *Biomed. Chromatogr.* **2009**, *23*, 951–965.
(16) Dunn, W. B.; Broadhurst, D.; Brown, M.; Baker, P. N.; Redman, C. W. G.; Kenny, L. C.; Kell, D. B. *J. Chromatogr., B* **2008**, *871*, 288–298.
(17) Zhang, N. R.; Yu, S.; Tiller, P.; Yeh, S.; Mahan, E.; Emary, W. B. *Rapid Commun. Mass Spectrom.* **2009**, *23*, 1085–1094.
(18) Koulman, A.; Woffendin, G.; Narayana, V. K.; Welchman, H.; Crone, C.; Volmer, D. A. *Rapid Commun. Mass Spectrom.* **2009**, *23*, 1411–1418.
(19) Bateman, K. P.; Kellmann, M.; Muenster, H.; Papp, R.; Taylor, L. *J. Am. Soc. Mass Spectrom.* **2009**, *20*, 1441–1450.
(20) Kellmann, M.; Muenster, H.; Zomer, P.; Mol, H. *J. Am. Soc. Mass Spectrom.* **2009**, *20*, 1464–1476.
(21) Wishart, D. S.; Tzur, D.; Knox, C.; Eisner, R.; Guo, A. C.; Young, N.; Cheng, D.; Jewell, K.; Arndt, D.; Sawhney, S.; Fung, C.; Nikolai, L.; Lewis, M.; Coutouly, M. A.; Forsythe, I.; Tang, P.; Shrivastava, S.; Jeroncic, K.; Stothard, P.; Amegbey, G.; Block, D.; Hau, D. D.; Wagner, J.; Miniaci, J.; Clements, M.; Gebremedhin, M.; Guo, N.; Zhang, Y.; Duggan, G. E.; MacInnis, G. D.; Weljie, A. M.; Dowlatabadi, R.; Bamforth, F.; Clive, D.; Greiner, R.; Li, L.; Marrie, T.; Sykes, B. D.; Vogel, H. J.; Querengesser, L. *Nucleic Acids Res.* **2007**, *35*, D521–D526.
(22) Gutnick, D.; Calvo, J. M.; Klopotow., T; Ames, B. N. *J. Bacteriol.* **1969**, *100*, 215.
(23) Luo, B.; Groenke, K.; Takors, R.; Wandrey, C.; Oldiges, M. *J. Chromatogr., A* **2007**, *1147*, 153–164.
(24) Lu, W.; Bennett, B. D.; Rabinowitz, J. D. *J. Chromatogr., B* **2008**, *871*, 236–242.
(25) Buscher, J. M.; Czernik, D.; Ewald, J. C.; Sauer, U.; Zamboni, N. *Anal. Chem.* **2009**, *81*, 2135–2143.

falling outside of the scan range are selected against. Empirically, we found that this selection was adequate to substantially improve the analytical results. Later in the LC run, the lower m/z limit was raised yet higher, as low molecular weight metabolites elute early in this reversed phase LC method. The final MS scan method is thus made in the following with segments: 0−5 min, m/z 85−800; 5−6.7 min, m/z 100−800; 6.7−9 min, m/z 85−800; 9−16 min, m/z 110−1000; 16−24 min, m/z 220−1000. The last minute in the LC run is for column equilibrium only and is not scanned. Other MS method settings are resolution 100 000 at 1 Hz (1 scan per second), AGC (automatic gain control) target 3×10^6, maximum injection time 100 μS.

Method Validation for Purified Metabolites. Method performance was evaluated for 87 metabolite standards (Supporting Information, Table S-1) with respect to limit of detection (LOD), linearity, reproducibility, and mass accuracy. For each purified metabolite, ≥ 0.1 mg/mL stock solution was prepared in 50:50 methanol/water and stored at −80 °C. From these stock solutions, mixtures of ∼10 metabolites dissolved in water were prepared at 1, 2, 5, 10, 20, 50, 100, 200, 500, 1000, 2000 ng/mL and analyzed. LOD was defined as the lowest concentration at which the signal is at least 3-fold of the corresponding background. Linearity was evaluated using the linear regression of the observed signal with respect to concentration, with the lower limit always being the LOD. In the case that LOD was >100 ng/mL, secondary experiments were done using standards at 200, 500, 1000, 2000, 5000, 10 000 ng/mL to determine the linear range. In addition, standards at 100 ng/mL were run four times to determine inter-run, intraday quantitative reproducibility, as measured by the relative standard deviation (RSD). Mass accuracy was determined based on parts per million error, defined as [(measured mass − theoretical mass)/theoretical mass] × 10^6, and was evaluated at 100 ng/mL (or 1000 ng/mL for compounds with LOD > 100 ng/mL).

For LC−MS-based targeted metabolomics, it is desirable to detect as many metabolites as possible using their retention times and accurate masses. After verifying that the current method works well for 87 metabolites, we determined the retention time for an additional 127 metabolites using their standards at a concentration of ∼1 μg/mL. This resulted in a list of 214 known metabolites that can be detected by this method (Tables S-1 and S-2 in the Supporting Information). The number of known metabolites that can be detected is largely limited by the availability of the purified standards.

Yeast Culture and Extraction. *S. cerevisiae* auxotrophic strains carrying deletion alleles of the candidate gene *ykl215C*Δ::*kanMX* and the control mutant *yar047C*Δ::*kanMX* were freshly derived by haploid selection from sporulated cultures of systematic yeast SGA deletion strains (Open Biosystems). A prototrophic *ykl215C*Δ::*kanMX* yeast strain was derived from a cross with FY5, and compared to FY5.[26] A saturated overnight culture was set back to an optical density at 600 nm (OD_{600}) of 0.1 in 25 mL of liquid culture media. After approximately two doublings (OD_{600} = 0.4), the 25 mL culture was rapidly filtered and the filter-bound cells quenched by immediately dropping them into 0.8 mL of −20 °C extraction solvent (40:40:20 acetonitrile/methanol/water). The quenched cells (with the filter still present) were then extracted at −20 °C for 15 min, then residual cells were washed from the filter with 0.2 mL solvent, and the filter discarded. The resulting mixture of cell debris and extraction solvent was transferred to a 1.5 mL eppendorf tube and centrifuged at 13 200 rpm for 5 min at 4 °C. The supernatant was removed and stored at 4 °C. The pellet was resuspended in 0.2 mL extraction solvent and allowed to sit at 4 °C for 15 min, followed by centrifugation at 13 200 rpm for 5 min at 5 °C. The two supernatants were combined, dried under nitrogen flow on an N-EVAP nitrogen evaporator (Organomation Associates, Berlin, MA), and resuspended in 1.2 mL of water to yield a sample ready for LC−MS analysis. In all cases, data shown are for FY4, with FY5 yielding similar results.

For experiments involving determination of the carbon- and nitrogen-counts in unknown metabolites, yeast were grown in unlabeled media, as well as in [U-^{13}C]-glucose, ^{15}N-ammonia, and [U-^{13}C]-glucose plus ^{15}N-ammonia labeled media for a minimum of 12 doublings, yielding "heavy" metabolites. The difference in mass between the "heavy" and "light" metabolite correlates with the number of carbons or nitrogens in the molecule.

^{13}C-Isotope Labeling of Metabolites in *Escherichia coli*. To test the suitability of the current method for the study of metabolic flux, we studied the ^{13}C-isotope labeling pattern of selected metabolites from *E. coli*, when switched from normal glucose (with natural isotope contribution of 98.9% of ^{12}C and 1.1% of ^{13}C) to uniformly ^{13}C-labeled glucose as the carbon source. The *E. coli* strain used was NCM3722. For its culture, we used a filter-based approach that allows for rapid switching of media, as described previously.[27,28] In brief, the cells are transferred by filtration to the surface of a filter, which is placed on an agarose support. The cells grow on the filter surface at a rate similar to that in liquid media, fed by diffusion of nutrients through the agarose and filter. Media composition (in this case from unlabeled to uniformly ^{13}C-labeled glucose media) can then be quickly varied by moving the filter-bound cells from one agarose plate to another. All experimental details are as per Yuan et al.,[29] with the following exceptions: filter size was reduced from 82 to 47 mm; all liquid volumes (for filter loading and extraction) were correspondingly reduced 3-fold; and the final supernatants were dried and redissolved in 300 μL of water prior to analysis by LC−MS. The signals of the ^{13}C-labeled forms were corrected for the natural isotope abundance of the unlabeled glucose as described previously.[30] Similar results to those shown for *E. coli* have also been obtained from *S. cerevisiae*.

Data Analysis. High-resolution mass spectrometers have the potential to quantitate known analytes (targeted analysis) while simultaneously collecting untargeted data on all ions present, including ones arising from unanticipated compounds (untargeted analysis). The raw data files can be analyzed using the standard data analysis software provided by the vendor (Xcalibur), looking

(26) Winston, F.; Dollard, C.; Ricupero-Hovasse, S. L. *Yeast* **1995**, *11*, 53–55.
(27) Yuan, J.; Fowler, W. U.; Kimball, E.; Lu, W. Y.; Rabinowitz, J. D. *Nat. Chem. Biol.* **2006**, *2*, 529–530.
(28) Brauer, M. J.; Yuan, J.; Bennett, B. D.; Lu, W. Y.; Kimball, E.; Botstein, D.; Rabinowitz, J. D. *Proc. Natl. Acad. Sci. U.S.A.* **2006**, *103*, 19302–19307.
(29) Yuan, J.; Bennett, B. D.; Rabinowitz, J. D. *Nat. Protoc.* **2008**, *3*, 1328–1340.
(30) Munger, J.; Bennett, B. D.; Parikh, A.; Feng, X. J.; McArdle, J.; Rabitz, H. A.; Shenk, T.; Rabinowitz, J. D. *Nat. Biotechnol.* **2008**, *26*, 1179–1186.

at the extracted ion chromatograms for every mass of interest; however, this is a slow process when analyzing a large number of samples and compounds. To facilitate data analysis, in-house software, mzROLL, was developed for semiautomated data processing. The software involves many of the same principles as the widely used XCMS code.[31] A brief description is presented here, with details to be published elsewhere.

Targeted Analysis. Thermo Fisher mass spectrometry RAW files were converted from the profile mode into the centroid mode using the ReAdW program.[32] Centroided files were loaded into mzROLL and aligned by fitting a high-degree polynomial to the retention times of the highest intensity ions across the samples. Extracted ion chromatograms (EICs) were extracted using a 5 ppm window centered on the expected m/z of each known compound and smoothed by applying a Gaussian filter to the signal intensity. Within each EIC, peaks were detected and the quality of all peaks was evaluated by a random forest based classification model that takes into account peak height, peak width, peak area, the signal-to-noise ratio, and the peak shape.[33] Peaks were grouped across samples and matched to the expected retention time of each compound. The peak closest to the expected retention time with an acceptable quality score was used for quantitation. All peaks used for quantitation were hand-checked after automated extraction and assignment. The isotopically labeled forms of compounds were extracted in a similar manner. Quantitation of labeled forms was based on the highest intensity peak within a 5 ppm window around the expected m/z of the ^{13}C- and/or ^{15}N-labeled form of the compound.

Untargeted Analysis. Ion-specific chromatograms are generated for all observed ion signals, using a 5 ppm m/z window, resulting in a large matrix with peaks as rows, samples as columns, and peak intensities as the entries. Statistically significant differences between mutant and wild type metabolite profiles are determined using a type III t test and $\log_2$ fold changes in peak area. Peaks are refined to remove those corresponding to different adduct ions, isotopic variants, and in-source fragmentation. A first-pass approach to identification of the resulting list of significantly different $[M - H]^-$ peaks involves searching of known metabolite databases, such as KEGG,[34] Metacyc,[35] and Human Metabolome Database[36] for compounds of the correct exact mass, with further constraints provided by carbon- and nitrogen-atom counts obtained via labeling experiments.

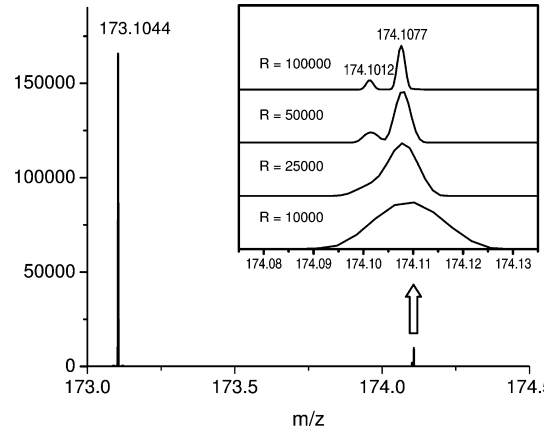

Figure 1. Negative ion mass spectrum of arginine standard at 10 μg/mL showing the base peak at m/z 173.1044, and its natural isotope peaks with one ^{15}N (m/z 174.1012) and one ^{13}C (m/z 174.1077). The latter two were not resolved at a resolution setting of 10 000 or 25 000, partially separated at 50 000, and well separated at 100 000.

RESULTS AND DISCUSSION

"Exactive" Overview. The "Exactive" is a stand-alone orbitrap mass spectrometer that is designed for high-resolution full scans. Ions formed by electrospray ionization are transferred to a curved linear trap (C-Trap), from which they are injected into the orbitrap for mass analysis. Mass resolution depends on scan speed. At m/z 200, resolution is 10 000 at 10 Hz; 25 000 at 4 Hz; 50 000 at 2 Hz; and 100 000 at 1 Hz. The effect of the Exactive's resolving power on analytical results has been demonstrated recently.[20] We find that the higher resolution settings offer important benefits, as they frequently help to separate overlapping ion peaks. As an example, Figure 1 shows the mass spectrum of arginine (purified standard), with a focus on the natural isotope peaks containing one ^{15}N nucleus (m/z 174.1012) versus one ^{13}C nucleus (m/z 174.1077). These two peaks merge at a resolution setting of 10 000 and 25 000, partially resolve at 50 000, and separate fully at 100 000. The Exactive's ability to separate ^{15}N- and ^{13}C-isotopomer peaks is useful for isotope tracer experiments.

Like any trap instrument, the performance of Exactive is affected by the space-charge effect.[37] If there are too many ions inside the trap, these will lead to distortion of the electric field and compromise the instrument performance. The Exactive has an automatic gain control function which controls the duration of ion injection into the orbitrap to maintain an optimum total number of ions (the AGC target value). When AGC is used, the instrument alternates between prescans and analytical scans. When the prescan finds a large total ion current (TIC), the injection time for the subsequent analytical scan is reduced. The user selects between three AGC target values: 3×10^6 for a high dynamic range scan, 1×10^6 for a balanced scan, and 5×10^5 for the best mass accuracy. Here we used the 3×10^6 target value to maximize quantitative performance, with the 5×10^5 target value useful for improving mass accuracy when aiming to identify unanticipated metabolites. To mitigate further the space-charge effect caused by anions in the cell culture media (phosphate and sulfate), we modulated the instrument's mo-

(31) Smith, C. A.; Want, E. J.; O'Maille, G.; Abagyan, R.; Siuzdak, G. *Anal. Chem.* **2006**, *78*, 779–787.

(32) Keller, A.; Eng, J.; Zhang, N.; Li, X. J.; Aebersold, R. *Mol. Syst. Biol.* **2005**, *1*, 8.

(33) Breiman, L. *Mach. Learn.* **2001**, *45*, 5–32.

(34) Kanehisa, M.; Araki, M.; Goto, S.; Hattori, M.; Hirakawa, M.; Itoh, M.; Katayama, T.; Kawashima, S.; Okuda, S.; Tokimatsu, T.; Yamanishi, Y. *Nucleic Acids Res.* **2008**, *36*, D480–D484.

(35) Caspi, R.; Foerster, H.; Fulcher, C. A.; Kaipa, P.; Krummenacker, M.; Latendresse, M.; Paley, S.; Rhee, S. Y.; Shearer, A. G.; Tissier, C.; Walk, T. C.; Zhang, P.; Karp, P. D. *Nucleic Acids Res.* **2008**, *36*, D623–D631.

(36) Wishart, D. S.; Knox, C.; Guo, A. C.; Eisner, R.; Young, N.; Gautam, B.; Hau, D. D.; Psychogios, N.; Dong, E.; Bouatra, S.; Mandal, R.; Sinelnikov, I.; Xia, J. G.; Jia, L.; Cruz, J. A.; Lim, E.; Sobsey, C. A.; Shrivastava, S.; Huang, P.; Liu, P.; Fang, L.; Peng, J.; Fradette, R.; Cheng, D.; Tzur, D.; Clements, M.; Lewis, A.; De Souza, A.; Zuniga, A.; Dawe, M.; Xiong, Y. P.; Clive, D.; Greiner, R.; Nazyrova, A.; Shaykhutdinov, R.; Li, L.; Vogel, H. J.; Forsythe, I. *Nucleic Acids Res.* **2009**, *37*, D603–D610.

(37) Cox, K. A.; Cleven, C. D.; Cooks, R. G. *Int. J. Mass Spectrom. Ion Processes* **1995**, *144*, 47–65.

lecular weight scan range to reduce accumulation of these ions in the orbitrap during the chromatographic internals where they elute (see Experimental Section for details).

LC−MS Method Development and Validation. Luo et al. originally described an LC−MS/MS method for metabolomics that coupled reversed phase HPLC with tributylamine as an ion-pairing reagent via electrospray ionization to triple quadrupole MS/MS.[23] The run time was 80 min. We subsequently modified the gradient to reduce the running time to 50 min.[24] The column particle size was 4 μm and the flow rate 200 μL/min. Although briefer than the original method of Luo et al., this method was still undesirably slow. Efforts to expedite analysis, however, ran up against the need for relatively slow compound elution to accommodate a large number of selected reaction monitoring scan events while retaining adequate coverage of individual chromatogram peaks. This is a typical problem when using triple-quadrupole instruments for "omic" analysis.

In the current method, we aimed to take advantage of the full scan capability of the Exactive orbitrap to expedite analysis. To this end, we selected a column particle size of 2.5 μm, which, without changing flow rate, enabled us to reduce the total running time to 25 min. Most of the resulting chromatogram peaks have a width of ~15 s, resulting in 15 data points across the peaks when scanning at 1 Hz (100 000 resolution). The maximum pump pressure during the LC run is ~300 bar, which can be obtained on high-quality HPLC systems, as well as UPLC systems.

In the Supporting Information, Table S-1, we summarize the results of the LC−MS method validation for 87 metabolite standards. The median limit-of-detection (LOD) is 5 ng/mL with 63 compounds (72%) having a LOD ≥ 10 ng/mL. The compounds with a higher LOD are mostly nucleotide di- and triphosphates and coenzyme A derivatives. All the compounds gave a linear response ($R^2 > 0.98$) over a concentration range of at least 10-fold, with 68 compounds (78%) showing an $R^2 > 0.98$ over at least a 100-fold concentration range. The quantitative reproducibility (intraday) was determined at a compound concentration of 100 ng/mL. For the 82 metabolites with an LOD ≤ 100 ng/mL, median RSD is 8.2% with 74 compounds (90%) showing a RSD < 20%.

We also evaluated mass accuracy using external calibration. For the 87 metabolites studied, 86 (99%) showed an error of <5 ppm with a median of −0.29. Mass accuracy is particularly good at the low mass region where most of compounds of interest appear. Mass accuracy can likely be further improved by using internal calibration.

Finally, we tested the method on an extract of Baker's yeast, *Saccharomyces cerevisiae*. We detected 137 known metabolites, with the observed signals (peak heights) as well as RSDs (intraday) listed in Table 1. The median RSD is 7.6%, indicating good reproducibility in real samples. Metabolites detected include amino acids, carboxylic acids, sugar phosphates, nucleotides, and coenzyme A derivatives, indicating the ability of the method to quantitate much of the core metabolome. Ion-specific chromatograms corresponding to selected metabolites are shown in Figure 2.

Kinetic Flux Profiling. With the switch from unlabeled to isotope-labeled nutrient, intracellular metabolites become labeled, with the rates of labeling depending on the proximity of the metabolite to the labeled nutrient in the metabolic network and the flux through the metabolite. Accordingly, labeling dynamics (kinetic flux profiling) can be used to probe metabolic network structures as well as to quantitate metabolic fluxes.[27,29] In our previous studies, this was done on a triple quadrupole mass spectrometer operating in multiple reaction monitoring (MRM) mode. When examining many metabolites, the MRM-based approach is cumbersome, especially for metabolites that can be partially labeled in many different ways, as each partially labeled form requires its own MRM scan. Moreover, selecting the appropriate product ion to monitor the partially labeled forms is not always straightforward.[27,38] With the use of high-resolution full scan MS, labeled metabolites can be identified based on their accurate masses. With this approach, we are able to monitor the labeling patterns of a large number of metabolites in parallel. Here we show results obtained upon switching *E. coli* from unlabeled to uniformly ^{13}C-labeled glucose for two representative compounds: fructose-1,6-bisphosphate (FBP) in glycolysis and citrate in the citric acid/tricarboxylic acid (TCA) cycle (Figure 3). Comparable quality of labeling data is obtained for most compounds. The full data, in tandem with relevant network-level analyses, will be described elsewhere.

Consistent with its position just downstream of glucose in the high-flux pathway of glycolysis, FBP labels quickly, with a half-time of ~2 min. Initially, FBP accumulates in two labeled forms: fully labeled and 3× ^{13}C-labeled. The fully labeled form is consistent with passage of glucose down glycolysis, whereas the three-labeled form is consistent with the reverse aldolase reaction joining together a fully labeled with an unlabeled triose phosphate (dihydroxyacetone phosphate or glycealdehyde-3-phosphate). The initial accumulation of three-labeled FBP at ≥50% of the rate of fully labeled FBP implies the reverse aldolase flux is a substantial fraction of the net glycolytic flux, i.e., that the aldolase reaction is near to equilibrium in glucose-fed *E. coli*. This observation is consistent with recent thermodynamic analysis of the glycolytic pathway.[39]

Citrate is a six-carbon metabolite formed by the condensation of the acetyl carbons of acetyl-CoA with the four-carbon TCA cycle compound oxaloacetate. Oxaloacetate can be generated in *E. coli* either by carboxylation of the three-carbon glycolytic compound phosphoenolpyruvate ("anapleurosis") or by turning of the TCA cycle. These sets of reactions lead to formation of citrate with 2, 3, 4, 5, or 6 labeled carbon atoms. Initially, 2× ^{13}C-labeling (from acetyl-CoA) and 3× ^{13}C-labeling (from anapleurosis) dominate, with subsequent rises in 4, 5, and 6 carbon labeling. After 30 min, the most abundant form is 5× ^{13}C-labeled, consistent with a 3× ^{13}C-labeled oxaloacetate (formed by the condensation of unlabeled carbon dioxide from the environment with labeled phosphoenolpyruvate) being joined with two labeled carbon atoms from acetyl-CoA. These data indicate that the anapleurotic flux in *E. coli* is larger than the flux associated with complete turning of the TCA cycle: complete turning of the TCA cycle would lead to 4× ^{13}C-labeling (from 2× acetyl-CoA) exceeding 3× ^{13}C-labeling and 5× ^{13}C-labeling (from anapleurosis) at early time points; similarly, complete turning of the

(38) Munger, J.; Bennett, B. D.; Parikh, A.; Feng, X. J.; McArdle, J.; Rabitz, H. A.; Shenk, T.; Rabinowitz, J. D. *Nat. Biotechnol.* **2008**, *26*, 1179–1186.
(39) Bennett, B. D.; Kimball, E. H.; Gao, M.; Osterhout, R.; Van Dien, S. J.; Rabinowitz, J. D. *Nat. Chem. Biol.* **2009**, *5*, 593–599.

Table 1. Retention Time, Mass Accuracy, Signal Intensity, And Quantitative Reproducibility for 137 Metabolites Detected from *Saccharomyces cerevisiae* Extract[a]

metabolite	neutral formula	theoretical mass	observed mass	mass error (ppm)	retention time (min)	signal (peak height)	RSD (%)
pyruvate	$C_3H_4O_3$	87.0088	87.0088	0.0	8.3	746 625	3.3
alanine	$C_3H_7NO_2$	88.0404	88.0404	0.0	1	67 324	13.3
4-aminobutyrate	$C_4H_9NO_2$	102.0561	102.0561	0.0	4.5	931 637	2.1
serine	$C_3H_7NO_3$	104.0353	104.0353	0.0	1	334 496	5.7
glycerate	$C_3H_6O_4$	105.0193	105.0194	1.0	6.3	23 659	28.4
proline	$C_5H_9NO_2$	114.0561	114.0561	0.0	1.12	68 602	9.4
fumarate	$C_4H_4O_4$	115.0037	115.0039	1.7	13.4	431 531	1.7
2-keto-isovalerate	$C_5H_8O_3$	115.0401	115.0402	0.9	13.06	482 462	1.9
indole	C_8H_7N	116.0506	116.0506	0.0	7.5	2 428	8.6
valine	$C_5H_{11}NO_2$	116.0717	116.0718	0.9	1	732 170	3.6
succinate	$C_4H_6O_4$	117.0193	117.0195	1.7	11.6	159 916	1.5
threonine/homoserine[a]	$C_4H_9NO_3$	118.051	118.051	0.0	1	625 574	10.8
cysteine	$C_3H_7NO_2S$	120.0125	120.0124	−0.8	1.1	2 531	14.3
nicotinate	$C_6H_5NO_2$	122.0248	122.0249	0.8	11.2	479 925	1.8
citraconic acid	$C_5H_6O_4$	129.0193	129.0196	2.3	12.95	501 333	4.1
hydroxyproline	$C_5H_9NO_3$	130.051	130.0509	−0.8	1.1	4 612	16.6
N-acetyl-L-alanine	$C_5H_9NO_3$	130.051	130.0511	0.8	7.97	36 010	3.1
leucine/isoleucine[a]	$C_6H_{13}NO_2$	130.0874	130.0874	0.0	1.9	459 288	9.4
oxaloacetate	$C_4H_4O_5$	130.9986	130.9986	0.0	13.64	999	11.9
asparagine	$C_4H_8N_2O_3$	131.0462	131.0462	0.0	1	345 435	7.7
hydroxyisocaproic acid	$C_6H_{12}O_3$	131.0714	131.0715	0.8	14.35	77 875	2.9
ornithine	$C_5H_{12}N_2O_2$	131.0826	131.0825	−0.8	1	1 799 867	10.4
aspartate	$C_{10}H_{16}N_2O_3S$	132.0302	132.0302	0.0	4.4	1 064 408	4.4
malate	$C_4H_6O_5$	133.0143	133.0145	1.5	12.7	638 679	1.1
homocysteine	$C_4H_9NO_2S$	134.0281	134.028	−0.7	1	5 919	8.8
p-aminobenzoate	$C_7H_7NO_2$	136.0404	136.0403	−0.7	8.7	1 756	21.3
p-hydroxybenzoate	$C_7H_6O_3$	137.0244	137.0245	0.7	10.88	3 153	8.7
acetylphosphate	$C_2H_5O_5P$	138.9802	138.9803	0.7	12.38	2 487	7
histidinol	$C_6H_{11}N_3O$	140.0829	140.0831	1.4	0.8	2 851	14.1
α-ketoglutarate	$C_5H_6O_5$	145.0143	145.0144	0.7	13.1	242 708	4
glutamine	$C_5H_{10}N_2O_3$	145.0619	145.0618	−0.7	1	7 112 816	6.3
lysine	$C_6H_{14}N_2O_2$	145.0983	145.0984	0.7	0.8	88 482	5.3
O-acetyl-L-serine	$C_5H_9NO_4$	146.0459	146.0456	−2.1	1.1	2 992	16.3
glutamate	$C_5H_9NO_4$	146.0459	146.0459	0.0	4.6	2 337 096	1
2-hydroxy-2-methylbutanedioic acid	$C_5H_8O_5$	147.0299	147.0302	2.0	12.6	440 951	6.3
methionine	$C_5H_{11}NO_2S$	148.0438	148.0438	0.0	1.6	158 639	6.4
hydroxyphenylacetic acid	$C_8H_8O_3$	151.0401	151.0403	1.3	14.8	1 541	9.1
histidine	$C_6H_9N_3O_2$	154.0622	154.0623	0.6	0.8	250 706	9.7
orotate	$C_5H_4N_2O_4$	155.0098	155.0101	1.9	8.1	8 437	13.6
dihydroorotate	$C_5H_6N_2O_4$	157.0255	157.0255	0.0	6.8	7 360	9.9
allantoin	$C_4H_6N_4O_3$	157.0367	157.0358	−5.7	0.82	32 477	5.2
indole-3-carboxylic acid	$C_9H_7NO_2$	160.0404	160.0406	1.2	14.4	8 789	6.4
aminoadipic acid	$C_6H_{11}NO_4$	160.0615	160.0615	0.0	4.33	43 651	3.3
phenylpyruvate	$C_9H_8O_3$	163.0401	163.0402	0.6	15.1	13 865	7.3
phenylalanine	$C_9H_{11}NO_2$	164.0717	164.0717	0.0	4.1	159 499	6.5
phenyllactic acid	$C_9H_{10}O_3$	165.0557	165.0559	1.2	14.82	20 423	7.4
quinolinate	$C_7H_5NO_4$	166.0146	166.0146	0.0	13.58	5 908	10.7
phosphoenolpyruvate	$C_3H_5O_6P$	166.9751	166.9752	0.6	13.7	6 117	1.8
pyridoxine	$C_8H_{11}NO_3$	168.0666	168.0667	0.6	1.8	83 996	15.1
D-glyceraldehdye-3-phosphate	$C_3H_7O_6P$	168.9908	168.9907	−0.6	7.3	7 245	5.7
dihydroxyacetone phosphate (DHAP)	$C_3H_7O_6P$	168.9908	168.9908	0.0	9.3	69 141	3
sn-glycerol-3-phosphate	$C_3H_9O_6P$	171.0064	171.0065	0.6	7.3	291 568	3.9
aconitate	$C_6H_6O_6$	173.0092	173.0092	0.0	13.8	160 846	6.8
N-acetyl-L-ornithine	$C_7H_{14}N_2O_3$	173.0932	173.093	−1.2	1	249 359	9.9
arginine	$C_{10}H_{14}N_5O_7P$	173.1044	173.1045	0.6	0.8	240 015	13
citrulline	$C_6H_{13}N_3O_3$	174.0884	174.0882	−1.1	0.9	2 308 219	9.4
N-carbamoyl-L-aspartate	$C_5H_8N_2O_5$	175.036	175.0363	1.7	12.6	34 300	2.7
2-isopropylmalic acid	$C_7H_{12}O_5$	175.0612	175.0613	0.6	13.94	2 251 182	1.9
glucono-δ-lactone	$C_6H_{10}O_6$	177.0405	177.0406	0.6	6.59	54 726	13.9
hydroxyphenylpyruvate	$C_9H_8O_4$	179.035	179.0351	0.6	13.58	5 208	7.7
tyrosine	$C_9H_{11}NO_3$	180.0666	180.0667	0.6	2	23 290	11.4
3-phospho-serine	$C_3H_8NO_6P$	184.0017	184.0017	0.0	8.2	2 789	10.1
3-phosphoglycerate	$C_3H_7O_7P$	184.9857	184.9859	1.1	13.58	113 737	30.2
N-acetyl-glutamine	$C_7H_{12}N_2O_4$	187.0724	187.0725	0.5	7	374 275	1.9
acetyllysine	$C_8H_{16}N_2O_3$	187.1088	187.1089	0.5	1.2	120 124	4.2
kynurenic acid	$C_{10}H_7NO_3$	188.0353	188.0353	0.0	14.22	5 987	9.8
N-acetyl-glutamate	$C_7H_{11}NO_5$	188.0564	188.0567	1.6	13	956 618	3.3
citrate/isocitrate[a]	$C_6H_8O_7$	191.0197	191.0198	0.5	13.6	1 350 132	0.7
2-dehydro-D-gluconate	$C_6H_{10}O_7$	193.0354	193.0354	0.0	5	3 770	4.8
D-gluconate	$C_6H_{12}O_7$	195.051	195.0511	0.5	5.8	210 301	4.8
D-erythrose-4-phosphate	$C_4H_9O_7P$	199.0013	199.0014	0.5	7.45	23 954	6.7

Table 1. Continued

metabolite	neutral formula	theoretical mass	observed mass	mass error (ppm)	retention time (min)	signal (peak height)	RSD (%)
tryptophan	$C_{11}H_{12}N_2O_2$	203.0826	203.0826	0.0	7.6	47 267	3.2
xanthurenic acid	$C_{10}H_7NO_4$	204.0302	204.0304	1.0	13.9	9 495	15.5
D-glucarate	$C_6H_{10}O_8$	209.0303	209.0305	1.0	13	627	28.7
pantothenate	$C_9H_{17}NO_5$	218.1034	218.1035	0.5	11	504 663	3.1
cystathionine	$C_7H_{14}N_2O_4S$	221.0602	221.0598	−1.8	1	29 616	4.4
ribose-5-phosphate	$C_5H_{11}O_8P$	229.0119	229.0119	0.0	7.2	103 275	3.7
cytidine	$C_9H_{13}N_3O_5$	242.0783	242.0782	−0.4	1.2	1 704	27
uridine	$C_9H_{12}N_2O_6$	243.0623	243.0622	−0.4	2.1	79 656	3.7
biotin	$C_{10}H_{16}N_2O_3S$	243.0809	243.0811	0.8	12.6	3 822	9
shikimate-3-phosphate	$C_7H_{11}O_8P$	253.0119	253.0121	0.8	13.44	25 262	7.2
D-glucono-δ-lactone-6-phosphate	$C_6H_{11}O_9P$	257.0068	257.0068	0.0	6.17	4 570	14
D-glucosamine-1/6-phosphate[a]	$C_6H_{14}NO_8P$	258.0384	258.0387	1.2	1.5	6 274	29.8
fructose-6-phosphate	$C_6H_{13}O_9P$	259.0224	259.0225	0.4	7.3	67 097	4.6
glucose-6-phosphate	$C_6H_{13}O_9P$	259.0224	259.0225	0.4	6.9	594 878	1.9
thiamine	$C_{12}H_{16}N_4OS$	263.0972	263.0973	0.4	0.8	404 390	9.9
2,3-diphosphoglycerate	$C_3H_8O_{10}P_2$	264.952	264.9522	0.8	14.68	48 631	3.3
inosine	$C_{10}H_{12}N_4O_5$	267.0735	267.0736	0.4	3.6	5 219	14.1
6-phospho-D-gluconate	$C_6H_{13}O_{10}P$	275.0174	275.0176	0.7	13.38	249 507	2.8
1-methyladenosine	$C_{11}H_{15}N_5O_4$	280.1051	280.104	−3.9	1	1 031	32.1
guanosine	$C_{10}H_{13}N_5O_5$	282.0844	282.0845	0.4	4.2	1 155	2
S-methyl-5′-thioadenosine	$C_{11}H_{15}N_5O_3S$	296.0823	296.0828	1.7	11.6	1 123	21.9
7-methylguanosine	$C_{11}H_{16}N_5O_5$	297.1079	297.1068	−3.7	1.16	1 104	19.2
N-acetyl-D-glucosamine-1/6-phosphate[a]	$C_8H_{16}NO_9P$	300.049	300.0492	0.7	7.3	27 244	1.4
glutathione	$C_{10}H_{17}N_3O_6S$	306.0765	306.0766	0.3	8	2 002 776	2.9
thymidine-5′-phosphate (dTMP)	$C_{10}H_{15}N_2O_8P$	321.0493	321.0496	0.9	11.27	1 640	12.9
cytidine-5′-phosphate (CMP)	$C_9H_{14}N_3O_8P$	322.0446	322.0451	1.6	8.7	1 944	17.1
uridine-5′-monophosphate (UMP)	$C_9H_{13}N_2O_9P$	323.0286	323.0291	1.5	10.2	8 410	13.1
3′,5′-cyclic AMP	$C_{10}H_{12}N_5O_6P$	328.0453	328.0458	1.5	12.6	3 287	10.6
fructose-1,6-bisphosphate	$C_6H_{14}O_{12}P_2$	338.9888	338.9891	0.9	13.5	1 405 676	5.6
trehalose/sucrose/cellobiose[a]	$C_{12}H_{22}O_{11}$	341.109	341.1089	−0.3	1.18	80 239	8.8
adenosine-5′-phosphate (AMP)	$C_{10}H_{14}N_5O_7P$	346.0558	346.0562	1.2	11.3	35 081	7.6
inosine-5′-phosphate (IMP)	$C_{10}H_{13}N_4O_8P$	347.0398	347.0403	1.4	10.7	13 453	9.2
guanosine-5′-phosphate (GMP)	$C_{10}H_{14}N_5O_8P$	362.0507	362.0512	1.4	10.7	10 006	4.8
xanthosine-5-phosphate	$C_{10}H_{13}N_4O_9P$	363.0347	363.0356	2.5	12.7	2 887	8.6
orotidine-5′-phosphate	$C_{10}H_{13}N_2O_{11}P$	367.0184	367.0188	1.1	13.58	1 278	25.8
riboflavin	$C_{17}H_{20}N_4O_6$	375.131	375.1319	2.4	12.2	885	6.2
S-adenosyl-L-homocysteine	$C_{10}H_{12}N_5O_6P$	383.1143	383.1149	1.6	6.1	10 200	11
5-phosphoribosyl-1-pyrophosphate	$C_5H_{13}O_{14}P_3$	388.9446	388.9452	1.5	14.94	27 112	7.7
thymidine-5′-diphosphate (dTDP)	$C_{10}H_{16}N_2O_{11}P_2$	401.0157	401.0161	1.0	13.58	1 430	40.7
cytidine-5′-diphosphate (CDP)	$C_9H_{15}N_3O_{11}P_2$	402.0109	402.0115	1.5	13.3	7 945	12.3
uridine-5′-diphosphate (UDP)	$C_9H_{14}N_2O_{12}P_2$	402.9949	402.9952	0.7	13.5	31 368	4
trehalose-6-phosphate	$C_{12}H_{23}O_{14}P$	421.0753	421.0757	0.9	7.2	21 367	12.1
adenosine-5′-diphosphate (ADP)	$C_{10}H_{15}N_5O_{10}P_2$	426.0221	426.0227	1.4	13.7	170 373	4.5
guanosine-5′-diphosphate (GDP)	$C_{10}H_{15}N_5O_{11}P_2$	442.0171	442.0174	0.7	13.5	28 920	7
CDP-ethanolamine	$C_{11}H_{20}N_4O_{11}P_2$	445.0531	445.0536	1.1	6.38	3 180	12
flavin mononucleotide (FMN)	$C_{17}H_{21}N_4O_9P$	455.0974	455.0981	1.5	14.2	13 753	6.6
dCTP	$C_9H_{16}N_3O_{13}P_3$	465.9823	465.9829	1.3	14.8	6 439	7.6
thymidine 5′-triphosphate (dTTP)	$C_{10}H_{17}N_2O_{14}P_3$	480.982	480.9824	0.8	14.94	38 064	9.2
cytidine-5′-triphosphate (CTP)	$C_9H_{16}N_3O_{14}P_3$	481.9772	481.9779	1.5	14.8	160 273	7.7
uridine-5′-triphosphate (UTP)	$C_9H_{15}N_2O_{15}P_3$	482.9612	482.9619	1.4	15	989 523	6.8
dATP	$C_{10}H_{16}N_5O_{12}P_3$	489.9936	489.9941	1.0	14.94	9 053	10.2
adenosine-5′-triphosphate (ATP)	$C_{10}H_{16}N_5O_{13}P_3$	505.9885	505.9889	0.8	15.1	1 449 520	5
guanosine-5′-triphosphate (GTP)	$C_{10}H_{16}N_5O_{14}P_3$	521.9834	521.9839	1.0	15	170 050	8.2
UDP-D-glucose	$C_{15}H_{24}N_2O_{17}P_2$	565.0477	565.0482	0.9	13.25	670 930	3.1
UDP-*N*-acetyl-glucosamine	$C_{17}H_{27}N_3O_{17}P_2$	606.0743	606.0748	0.8	13.27	1 159 364	2.9
glutathione disulfide	$C_{20}H_{32}N_6O_{12}S_2$	611.1447	611.1458	1.8	12.8	142 342	8.6
nicotinamide adenine dinucleotide (NAD^+)	$C_{21}H_{27}N_7O_{14}P_2$	662.1019	662.1024	0.8	8.6	529 138	2.4
nicotinamide adenine dinucleotide reduced (NADH)	$C_{21}H_{29}N_7O_{14}P_2$	664.1175	664.1187	1.8	13.9	5 125	10.3
dephospho-CoA	$C_{21}H_{35}N_7O_{13}P_2S$	686.1416	686.1451	5.1	14.8	623	18.9
nicotinamide adenine dinucleotide phosphate ($NADP^+$)	$C_{21}H_{28}N_7O_{17}P_3$	742.0682	742.0687	0.7	13.5	20 534	8.3
nicotinamide adenine dinucleotide phosphate reduced (NADPH)	$C_{21}H_{30}N_7O_{17}P_3$	744.0838	744.0845	0.9	14.87	57 597	7.3
coenzyme A	$C_{21}H_{36}N_7O_{16}P_3S$	766.1079	766.1079	0.0	15.5	3 194	28.1
flavin adenine dinucleotide (FAD)	$C_{27}H_{33}N_9O_{15}P_2$	784.1498	784.1503	0.6	15	16 629	9.5
acetyl-CoA	$C_{23}H_{38}N_7O_{17}P_3S$	808.1185	808.119	0.6	15.6	103 422	13.9
malonyl-coA	$C_{24}H_{38}N_7O_{19}P_3S$	852.1083	852.1105	2.6	15.6	2 979	11.8
3-hydroxy-3-methylglutaryl-CoA	$C_{27}H_{44}N_7O_{20}P_3S$	910.1502	910.1516	1.5	15.72	5 296	4.9

[a] Indicates structural isomers that are not separated with current method.

TCA cycle would lead to complete citrate labeling (rather than five carbon labeling) at late time points.

Discovery Metabolite Profiling. Even for well-studied organisms like *E. coli* and yeast, the functions of many genes remain unknown. For metabolic enzymes, comparison of the metabolome of wild-type and gene deletion strains provides a powerful tool for gene function elucidation. Enzyme knockout typically leads to the elevation of the enzyme's substrates and/

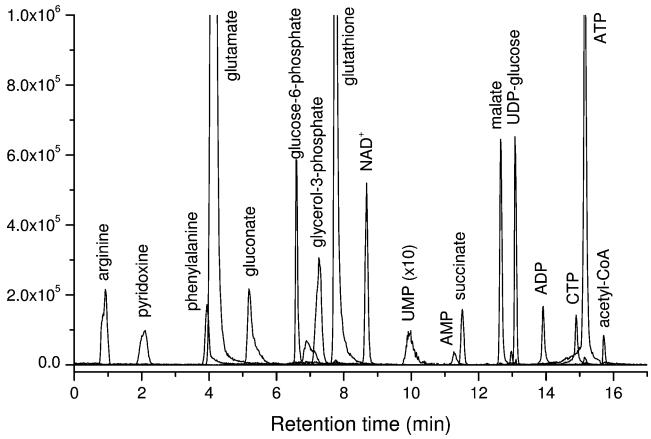

Figure 2. Overlay of extracted ion chromatograms of selective metabolites from a *S. cerevisiae* extract.

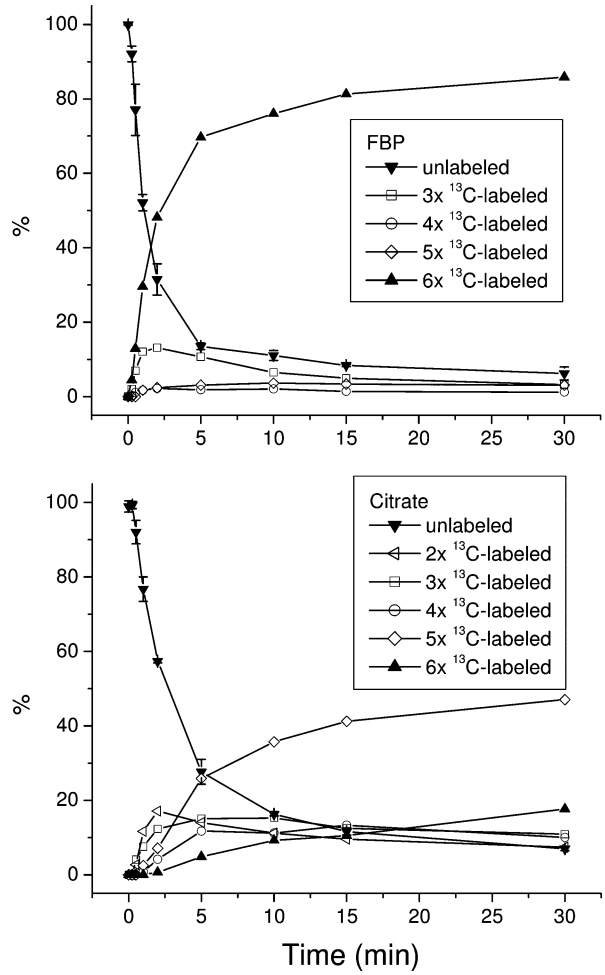

Figure 3. Relative labeling percentage of two representative metabolites as a function of time: fructose-1,6-bisphosphate (FBP, top panel), and citrate (bottom panel). For the purpose of simplicity, the following labeled forms are not plotted: $^{13}C_1$- and $^{13}C_2$-labeled FBP which have a maximum percentage of 1.7% and 1.4%, respectively, and $^{13}C_1$-labeled citrate which has a maximum percentage of 1.3%. The standard deviations for $N = 2$ are shown for the unlabeled forms.

or the depletion of its products. This approach has been previously used to assign enzyme functions in mammals.[40] Its

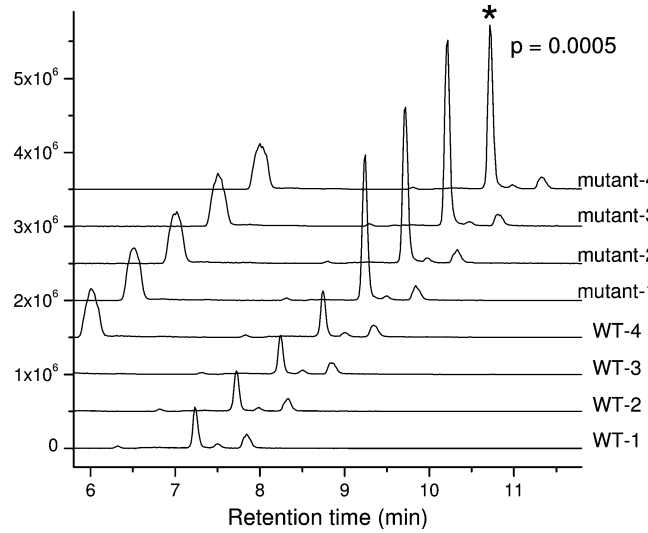

Figure 4. Chromatogram traces of *m/z* slice 128.0347−128.0360 (128.0353 ± 5 ppm) from extracts of wild type yeast and *YKL215C (oxp1)* deletion mutant yeast (each with four biological replicates). The replicates of the same strain give similar results, while there is a >3-fold difference for the features at 7.2 min between the WT and mutant strains ($p = 0.0005$ by *t* test). The feature was identified as 5-oxoproline (see text for details).

success relies on having an analytical method for metabolome profiling which is adequate to quantitate the enzyme's substrates and/or products. The method should preferably be untargeted, to enable discovery also of novel metabolites, enzymatic activities, and pathways.

Here we used the present LC−MS method to investigate the function of the gene *YKL215C*, whose role in yeast was previously unknown. Untargeted metabolite profiling of extracts of the wild type and knockout strains revealed >10 000 mass spectral features. Three *m/z* features with ≥3-fold differences between all mutant and control strains were identified, each of which appeared at the same retention time, 7.2 min, with the strongest signal associated with *m/z* 128.0351 (Figure 4). The other two features are at *m/z* 279.0593 and *m/z* 355.0454, with a relative signal intensity of 10% and 0.7% of the feature at *m/z* 128.0351. When searched against the KEGG database, the compound with *m/z* 128.0351 in negative ion mode matched the exact mass of 5-oxoproline (neutral formula $C_5H_6NO_3$, *m/z* 128.0353 in negative mode) with <2 ppm mass accuracy.

Additional experiments were performed to confirm the compound's identity. First, when fed [U-^{13}C]-glucose or ^{15}N-ammonia, we observed the disappearance of the ion *m/z* 128.0351. Instead, at the same retention time, we observed the accumulation of ions with *m/z* 133.0516 and *m/z* 129.0317, respectively. The masses match those of 5× ^{13}C oxoproline (expected *m/z* 133.0521, 3.8 ppm error), and 1× ^{15}N oxoproline (expected *m/z* 129.0323, 4.6 ppm error), consistent with 5-oxoproline containing five carbons and one nitrogen. Second, we spiked the cellular extracts with authentic standard of 5-oxoproline at concentrations of 0.5 and 2.5 μg/mL. The peak signal corresponding to *m/z* 128.0351 with a retention time of 7.2 min increased with the concentration of standard added.

The other compounds that were elevated in the *YKL215C* deletion strain had exact masses of *m/z* 279.0593 and *m/z* 355.0454, and both

(40) Saghatelian, A.; Cravatt, B. F. *Nat. Chem. Biol.* **2005**, *1*, 130–142.

Table 2. Comparison of Triple Quadrupole MS/MS and "Exactive" Orbitrap Full Scan MS for Metabolomics

features	triple quadrupole MS	"exactive" Orbitrap MS
detection mechanism	multiple reaction monitoring (MS/MS)	high-resolution accurate mass
preoptimization	required to find the product ions and best collision energy	not required
no. of detectable compounds	limited	virtually unlimited
untargeted analysis	no	yes
unknown metabolite identification	possible, through MS/MS fragmentation	possible, through accurate mass
UPLC compatibility	sometimes challenging due to requirement for adequate chromatographic time for MRM scans	yes
sensitivity[a]	typical LOD in low ng/mL range	typical LOD in low ng/mL range
dynamic range[a]	mostly over 2−3 orders of magnitude	mostly over 2−3 orders of magnitude
reproducibility[a]	typical RSD of 10%	typical RSD of 10%

[a] On the basis of results obtained using Thermo instruments in our laboratory; results with other instruments and methods may vary.

coeluted with 5-oxoproline but with smaller ion intensity. Both also increase upon the addition of the 5-oxoproline standard to a metabolite extract, consistent with their being adducts of 5-oxoproline, although we remain unsure of their precise identities.

On the basis of these data, we hypothesized that *YKL215C* is an oxoprolinase. Consistent with this, subsequent investigation revealed that *YKL215C* shares 48% sequence identity to the verified *M. musculus* ATP-hydrolyzing 5-oxoprolinase (gene name Oplah). On the basis of these results, and following the nomenclature of the oxoprolinase genes in plants, we have registered the gene name in the Saccharomyces Genome Database (SGD) as OXP1. Thus, the present method has been successfully employed, without the need for MS/MS, for untargeted metabolite profiling, resulting in improved annotation of the genome of Baker's yeast.

Comparison with Triple-Quadrupole Instrument. The market price of the "Exactive" benchtop orbitrap instrument is comparable to that of modern triple-quadrupole instruments. Accordingly, a practical question regards their relative advantages and disadvantages for metabolomic analysis (Table 2). Both techniques are suitable for targeted analysis. Triple quadrupole instruments use MS/MS (multiple reaction monitoring, MRM) to achieve a high degree of analyte specificity, even in complex biological samples. On the downside, preoptimization is required to determine appropriate MRM parameters. The measured compounds are limited to those targeted by MRM events programmed in the method. In addition, quantitative performance decreases with an increasing number of MRM scan events, since each scan event takes a fixed time (so-called "scan time" or "dwell time").

The "Exactive" orbitrap mass analyzer, on the other hand, detects ions solely using high-resolution accurate mass. The high resolution is critical to obtaining adequate analyte specificity in complex biological samples without MS/MS. Preoptimization is not required. A generic full scan method can be used, looking for everything in the appropriate scan range. The number of compounds that can be detected is virtually unlimited. This is particularly useful when following many partially labeled metabolites in isotope tracer experiments. Quantitative performance is generally not affected by the number of metabolites to be detected, as long as the total number of ions entering the orbitrap at any given moment does not induce space charge effects.[37] A major advantage of the orbitrap is its usefulness also for untargeted analysis. While accurate mass alone is generally not sufficient to identify an unknown compound, it is a critical first step toward such a goal.

In our hands, the quantitative performance of both instrument types is similar. Both show sensitivity in the nanogram per milliliter range, linear response over 2−3 orders of magnitude, and reasonable reproducibility. Our finding that both instrument types offer similar quantitative performance for metabolomics is consistent with recent literature reaching a similar conclusion in the areas of pharmacokinetic analysis[19] and small molecule quantitation.[17]

In terms of specificity, each instrument type has its strengths and weaknesses. The orbitrap's high resolving power offers certain advantages compared to triple quadruple MS/MS. For example, lysine (m/z 145.0983) and glutamine (m/z 145.0619), which have very similar MS/MS spectra, can be distinguished without the need for LC separation based on their exact masses. Similarly, IMP (m/z 347.0398) can also be distinguished from $^{13}C_1$-labeled AMP (m/z 347.0592); as AMP is typically more abundant than IMP in cell extracts, this proves a practical virtue in metabolomic analysis even in the absence of isotope labeling. On the other hand, full scan alone can never distinguish isomers; a second dimension separation such as LC is needed. In contrast, it may be possible to distinguish isomers by MRM alone. For example, citrate can be detected using the selected reaction monitoring (SRM) transition m/z 191 ($C_6H_7O_7^-$) → 87 ($C_3O_3H_3^-$) at 18 eV, and isocitrate can be detected using SRM m/z 191 ($C_6H_7O_7^-$) → 117 ($C_4O_4H_5^-$) at 18 eV. Also, certain interferences can be better separated by MS/MS than exact mass. For example, in the present method, an unknown interference at m/z 89.0244 typically masks the signal for lactate (m/z 89.0244). Such cases highlight the utility of having multiple different MS techniques available.

CONCLUSIONS

A primary challenge in analytical method development in metabolomics is balancing comprehensiveness of metabolome coverage with quantitative performance. The present method, which couples reversed phase ion pairing chromatography on a small particle column with high-resolution full scan MS, is a step in this direction. Although limited to negative ion mode, the method is nevertheless suitable for the analysis of a broad range of core, water-soluble cellular metabolites. Its performance relies on the resolving power of the orbitrap mass analyzer, used here in stand-alone form, to separate targeted compounds from interfering peaks in complex cellular samples. This resolving power is also critical for enabling reliable analysis of specific isotopomers in samples rendered yet more complex by isotope labeling and for facilitating identification of untargeted metabolites. Applications of the method include quantitative metabolomics, fluxomics, and discovery metabolite profiling.

ACKNOWLEDGMENT

This research was supported by NIH Grant GM071508 for Center of Quantitative Biology at Princeton University. Additional support came from the Beckman Foundation, American Heart Association Grant 0635188N, NSF Career Award MCB-0643859, NIH Grant AI078063, and the DOE Biohydrogen program (to J.D.R.).

SUPPORTING INFORMATION AVAILABLE

Additional information as noted in text. This material is available free of charge via the Internet at http://pubs.acs.org.

Received for review December 14, 2009. Accepted March 8, 2010.

AC902837X